Electronic Supplementary Material (ESI) for Journal of Materials Chemistry C.
This journal is © The Royal Society of Chemistry 2022

Supporting Information

Role of crown ether in perovskite precursor for doctor-bladed perovskite solar cells: Investigated by liquid-phase scanning electron microscopy

Kuo-Wei Huang, Ming-Hsien Li, Po-Tsung Hsieh, Chen-Fu Lin, Raja Rajendran, Yung-Liang Tung, Peter Chen**

Experimental section:

Perovskite precursor preparation: The triple-cation-based perovskite precursor was delicately prepared inside an N_2-filled glovebox with ppm levels of oxygen and moisture. The formamidinium (FAI, GreatCell Solar) was prepared using a mixture of GBL (JT Baker), DMSO (JT Baker) and isopropanol (JT Baker) solution [R1]. Then, 0.159 M lead bromide ($PbBr_2$, TCI), 0.159 M methylammonium bormide (MABr, GreatCell Solar), 0.9 M lead iodide (PbI_2, TCI), 35 μL of CsI solution (1.35 M dissolved in DMSO) and 18-crown-6 (Sigma-Aldrich) were sequentially added. The perovskite precursor was heated at 70 °C and stored in a dark N_2-filled glovebox.

Device Fabrication: A fluorine-doped tin oxide (FTO) substrate (approximately 10 Ω per square, PILKINGTON) was cleaned sequentially with deionized (DI) water, ethanol, and acetone in an ultrasonic bath. An ultrathin TiO_2 blocking layer (b-TiO_2) was fabricated at less than 70 °C by employing the technique used in the published paper [R2]. The mesoporous TiO_2 (meso-TiO_2) layer was spin-coated using diluted TiO_2 paste (1:7 weight ratio of TiO_2 paste (DSL 30NRT, GreatCell Solar) to ethanol) on the b-TiO_2-coated substrate at 4000 rpm for 10 s. The meso-TiO_2 was dried on a hot plate at 120 °C for 10 min, followed by annealing at 500 °C for 60 min. Before depositing the perovskite, the substrate was treated with UV-Ozone for 10 min and preheated for 10 min on the blade track. The gap between the blade coater and the substrate was 225 μm. The operating temperature was 150 °C, and the blading speed was 30 mm/s. We used ceramic heaters (MAXTHERMO, 650 W) to post heat the top side of the perovskite film with a temperature of 110-115 °C. The distance between the ceramic heaters and the substrate was 5 cm. After the precursor solvent being evaporated, the perovskite film completed crystal growth and film formation on the track. Then, perovskite films moved to the self-design chamber to underwent vacuum-heat treatment at 85 °C. After that, the perovskite film was annealed for 1 h at 100 °C and then cooled to room temperature. For the hole transport material, a mixture comprising 72.3 mg of spiro-OMeTAD (Lumtec LT-S922), 35 μL of bis(trifluoromethane)sulfonamide lithium salt (Li-TFSI) solution (26 mg Li-TFSI in 100 μL ACN (> 98%, Alfa)), 28.8 μL of 4-tert-butylpyridne (tBp) (96%, Sigma), and 1 mL of chlorobenzene was prepared. Then the spiro-OMeTAD solution was bladed on the top of the perovskite film under ambient (RH: 40-45%). The gap between the blade coater and the substrate was 30 μm. The operating temperature was 60 °C, and the blading speed was 30 mm/s. Subsequently, 125 nm of gold was thermally evaporated on the spiro-OMeTAD layer as the top electrode for the PSCs under a pressure of 2.5×10^{-5} mbar.

Characterization: Scanning electron microscopy (SEM) images were obtained using a field-emission scanning electron microscope (ZEISS SUPRA™ 55VP; EDS mapping: AMETEK EDAX PV77-58120ME). Liquid-phase SEM (L-SEM) technology presented in this work was provided by Liquid View Technology. A micro capsule was used as the carrier for the perovskite precursor sample. The micro capsule was prepared by microelectromechanical systems (MEMS) to form a cavity for loading the sample. After placing the capsule on a fixed stage, the perovskite precursor sample could be loaded and sealed to avoid the leakage of solution. After preparing the liquid specimen, a conventional SEM microscope without modification of the SEM itself was used for such analysis. A JEOL JEM7001 SEM was used for the SEM image inspection, which was operated under the acceleration voltage of 30 kV. Field emission gun was used for the electron source and the resolution can be down to 1.5 nm at 15 kV. Fourier transform infrared (FT-IR) spectra were detected by a Thermo Nicolet spectrometer with a resolution of 4 cm^{-1}. The crystallographic structures of the perovskite films were determined through X-ray diffraction by using a Cu Kα line ($\lambda = 1.5418$ Å, D8, Bruker, Germany) at room temperature. Thermogravimetric analysis (TGA) was conducted using a PerkinElmer TGA 400 instrument under N_2 atmosphere. The heating rate was 10 °C/min from room temperature to 800 °C. The current density–voltage (*J–V*) curve characteristics of the devices were measured using a solar simulator (SS-F5-3A, Enlitech). The *J–V* curve was measured under 1 sun AM 1.5 G illumination (100 mW/cm^2, 300 W Xenon lamp). A calibrated silicon solar cell was used to adjust the light intensity.

References:

(R1) Huang, K.; Li, M.; Wu, S.; Chiu, P.; Chen, J.; Chen, Y.; Lin, C.; Tung, Y.; Chen, Peter; The Effects of Solvent on Doctor-Bladed Perovskite Light Absorber under Ambient Process Condition for Multiple-Cation Mixed Halide Perovskites. *Energy Technol.* **2021**, 9, 2000792.

(R2) Huang, K.; Chen, Y.; Li, M.; Wu, Y.; Chiu, P.; Lin, Y.; Tung, Y.; Tsai, S.; Chen, Peter; Low-temperature Growth of Uniform Ultrathin TiO_2 Blocking Layer for Efficient Perovskite Solar Cell. *Org. Electron.* **2019**, 75, 105379.

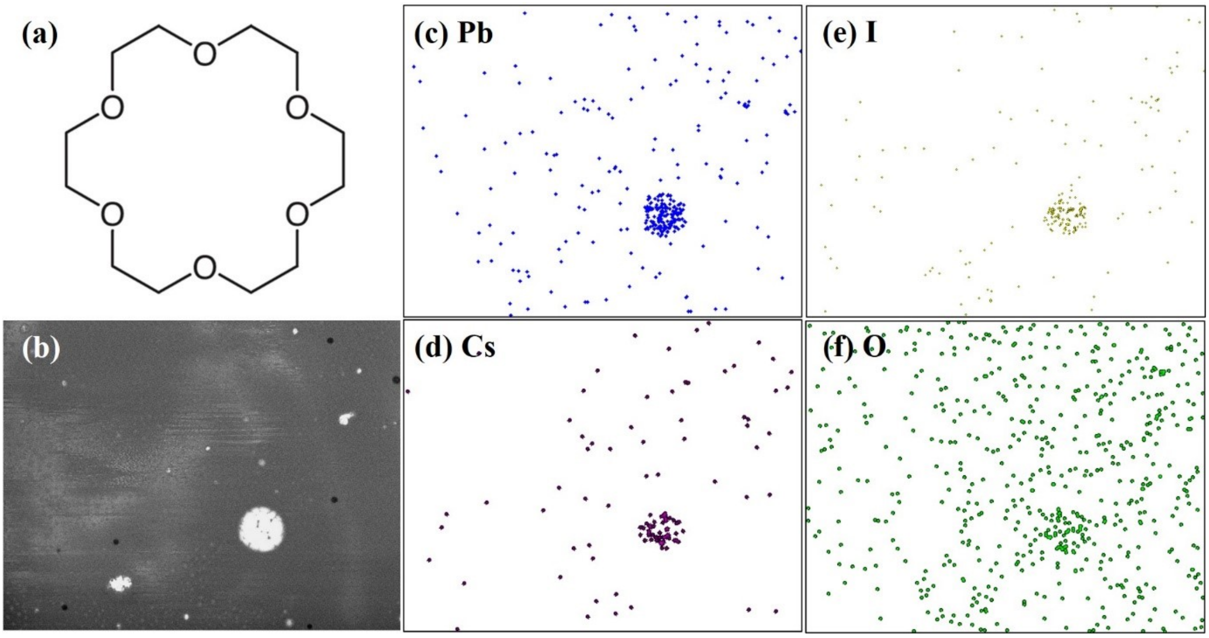

Figure S1. (a) Molecular structure of 18C6 crown ether. (b) L-SEM image, and EDX mapping of characteristic elements of (c) Pb, (d) Cs, (e) I and (f) O for MHP precursor with 0.95 mM 18C6.

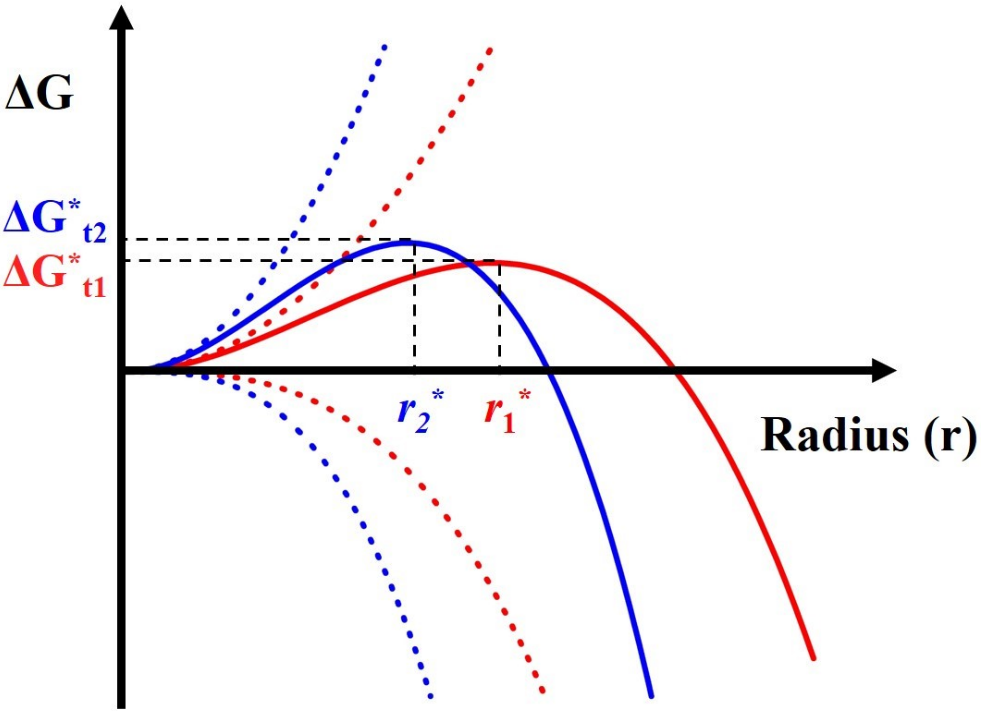

Figure S2. Change of free energy for nuclei formation as a function of nuclei radius.

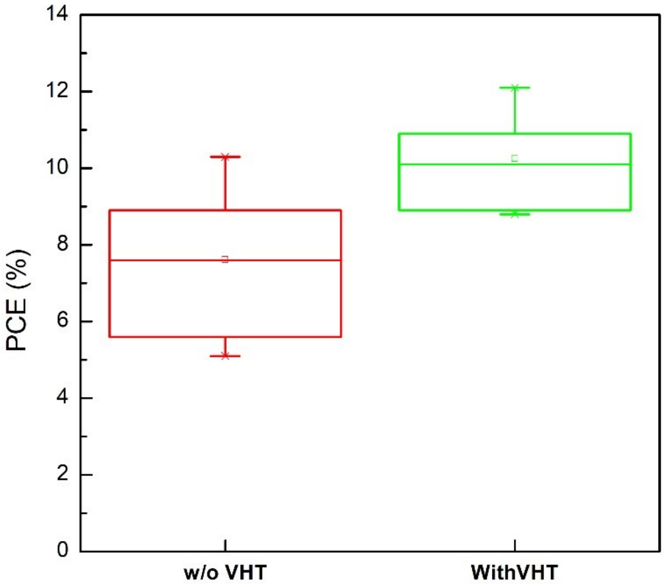

Figure S3. Statistic PCE for doctor-bladed PSCs with and without vacuum-heat treatment process.

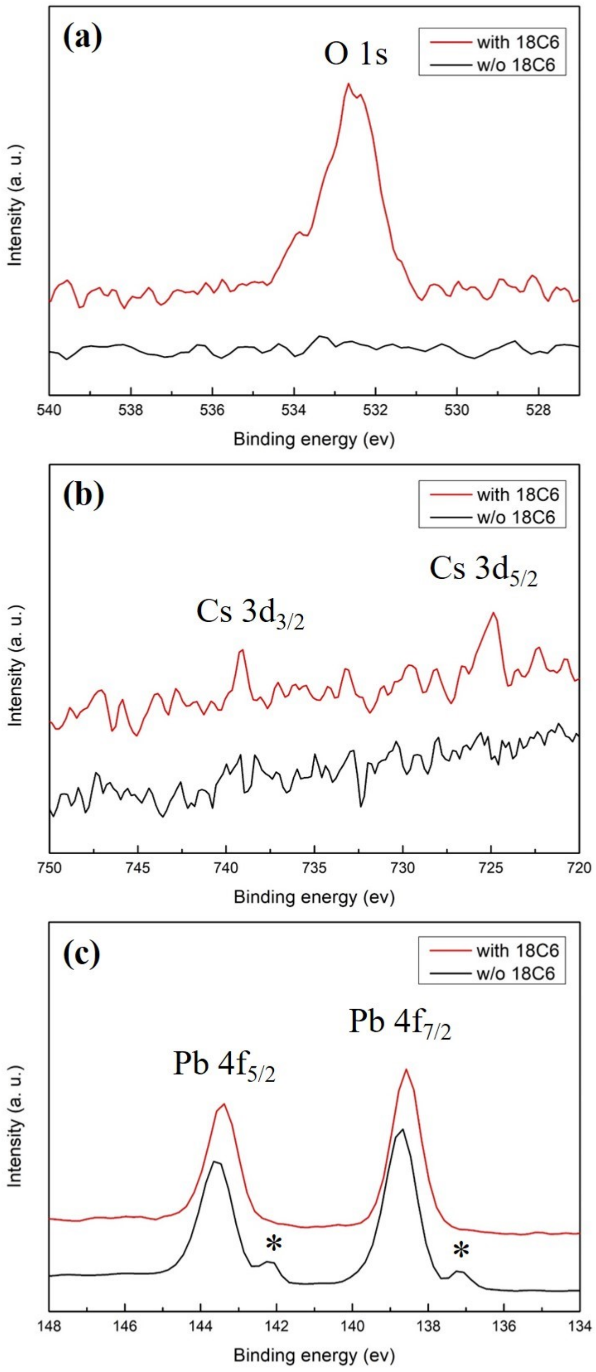

Figure S4. (a) O 1s, (b) Cs 3d, and (c) Pb 4f XPS spectra of MHP film without and with 0.95 mM 18C6.

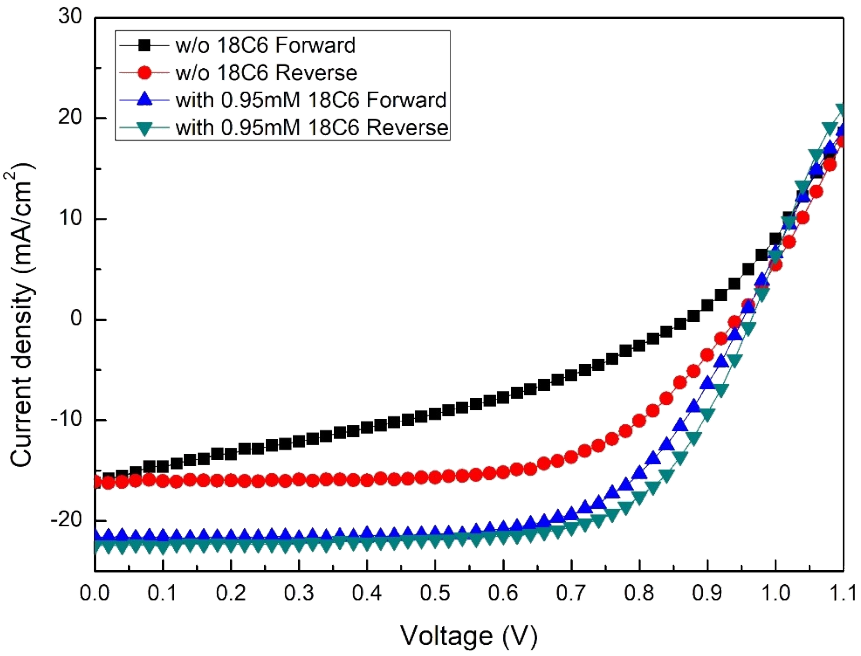

Figure S5. *J-V* curves of doctor-bladed PSCs with and without 0.95 mM 18C6 under forward and reverse scan.

Table S1. Normalized XRD peak ratio of (001), (002), and (003) facets of MHP films with different 18C6 concentration to the FTO.

18C6 concentration (mM)	(001)/FTO	(002)/FTO	(003)/FTO
0	2.36	2.57	1.17
0.05	2.95	3.22	1.45
0.25	5.44	6.40	1.36
0.45	4.46	5.07	1.56
0.95	19.55	37.93	8.74
1.9	6.66	8.81	1.97

Table S2. FWHM of (002) facet and corresponding mean grain size of MHP films with different 18C6 concentration.

18C6 concentration (mM)	FWHM	Mean grain size (nm)
0	0.192	426.2
0.05	0.175	467.7
0.25	0.122	670.8
0.45	0.125	654.7
0.95	0.087	940.7
1.9	0.101	810.3

Table S3. Best photovoltaic parameters of doctor-bladed PSCs made with different concentration of 18C6.

18C6 concentration (mM)	**V_{oc} (V)**	**J_{sc} (mA/cm^2)**	***FF* (%)**	**R_s (ohm)**	**R_{sh} (ohm)**	**HI**	**PCE (%)**
0	0.85	19.3	47.6	207.3	1719.2	0.74	7.8
0.25	0.88	19.5	57.6	208.4	29039.7	0.51	9.9
0.45	0.91	21.1	63.8	155.3	44573.4	0.14	12.3
0.95	0.96	22.4	67.9	131.9	52398.1	0.12	14.7
1.9	0.92	21.9	57.2	171.4	35996.3	0.23	11.7

Table S4. Calculated charge carrier lifetime of the MHP films with different concentration of 18C6.

18C6 concentration (mM)	**A_1**	**t_1 (ns)**	**A_2**	**t_2 (ns)**	**Average lifetime (ns)**
0	0.28	164.2	0.1	15.8	47.6
0.25	0.19	281.9	0.11	33.5	57.2
0.45	0.26	210.4	0.20	23.7	59.4
0.95	0.36	382.2	0.10	51.4	142.7
1.9	0.38	326.9	0.12	33.7	128.3

Table S5. Statistic photovoltaic parameters of doctor-bladed PSCs doped with 0.95 mM 18C6 under different active area.

Active area (cm^2)	**V_{OC} (V)**	**J_{SC} (mA/cm^2)**	**FF (%)**	**PCE (%)**
0.15	0.97 ± 0.01	21.4 ± 2.9	64.4 ± 4.5	13.4 ± 0.13
2.4	0.96 ± 0.01	17.1 ± 4.1	58.9 ± 9.6	9.7 ± 1.1